Available online at www.sciencedirect.com
ScienceDirect
Journal of Power Sources 172 (2007) 725–733
JOURNAL OF POWER SOURCES
www.elsevier.com/locate/jpowsour

Feasibility investigations on a novel micro-manufacturing process for fabrication of fuel cell bipolar plates: Internal pressure-assisted embossing of micro-channels with in-die mechanical bonding

Muammer Koç [a,*], Sasawat Mahabunphachai [a,b]

[a] *NSF I/UCR Center for Precision Forming (CPF), Department of Mechanical Engineering, Virginia Commonwealth University (VCU), Richmond, VA, USA*
[b] *Department of Mechanical Engineering, University of Michigan, Ann Arbor, MI, USA*

Received 21 March 2007; received in revised form 15 May 2007; accepted 17 May 2007
Available online 26 May 2007

Abstract

In this paper, we present the results of our studies on conceptual design and feasibility experiments towards development of a novel hybrid manufacturing process to fabricate fuel cell bipolar plates that consists of multi-array micro-channels on a large surface area. The premises of this hybrid micro-manufacturing process stem from the use of an internal pressure-assisted embossing process (cold or warm) combined with mechanical bonding of double bipolar plates in a single-die and single-step operation. Such combined use of hydraulic and mechanical forming forces and in-process bonding will (a) enable integrated forming of micro-channels on both surfaces (as anode and cathode flow fields) and at the middle (as cooling channels), (b) reduce the process steps, (c) reduce variation in dimensional tolerances and surface finish, (d) increase the product quality, (e) increase the performance of fuel cell by optimizing flow-field designs and ensuring consistent contact resistance, and (f) reduce the overall stack cost. This paper explains two experimental investigations that were performed to characterize and evaluate the feasibility of the conceptualized manufacturing process. The first investigation involved hydroforming of micro-channels using thin sheet metals of SS304 with a thickness of 51 μm. The width of the channels ranged from 0.46 to 1.33 mm and the height range was between 0.15 and 0.98 mm. Our feasibility experiments resulted in that different aspect ratios of micro-channels could be fabricated using internal pressure in a controllable manner although there is a limit to very sharp channel shapes (i.e., high aspect ratios with narrow channels). The second investigation was on the feasibility of mechanical bonding of thin sheet metal blanks. The effects of different process and material variables on the bond quality were studied. Successful bonding of various metal blanks (Ni201, Al3003, and SS304) was obtained. The experimental results from both investigations demonstrated the feasibility of the proposed manufacturing technique for making of the fuel cell bipolar plates.

Keywords: Fuel cell; Micro-manufacturing; Micro-channel; Hydroforming; Mechanical bonding

1. Introduction

Despite proven advantages such as high efficiency, quiet operations, and near-zero emissions, fuel cells are not yet cost competitive when compared to the existing power generation technologies, especially in the transportation applications. Compared to internal combustion engines, fuel cell power is 4–10 times more expensive ($30–50 kW^{-1} vs. $200–300 kW^{-1}) in its current status. Extensive research and development efforts are necessary to address the materials and manufacturing related technical issues to bring the cost of fuel cells down to competitive levels since around 60–70% of the fuel cell cost is in materials and manufacturing [1–5].

Among different components of the fuel cells, the bipolar plates stand as the high weight-, high volume-, and high cost-component (i.e., 60–80% of stack weight, 30–45% of stack cost [6,7]) with complicated micro-channels (in the range of 100–500 μm in depth and width) on both sides for effective distribution of hydrogen and oxygen gases, and inside cooling channels to sustain the operation temperature within 80–90 °C for efficient performance (i.e., 0.6–0.7 V per cell). The bipolar plates have also stringent requirements for electrical conduc-

* Corresponding author. Tel.: +1 804 827 7029; fax: +1 804 827 7030.
E-mail address: mkoc@vcu.edu (M. Koç).

0378-7753/$ – see front matter © 2007 Elsevier B.V. All rights reserved.
doi:10.1016/j.jpowsour.2007.05.089

tivity, corrosion resistance, weight, thickness, handling, etc. Basically, the bipolar plate needs to meet the following requirements (DOE Goals by 2010): (1) thin (<1 mm), (2) lightweight (<1 kg kW^{-1}), (3) high corrosion resistance (<1 μA cm^{-2}), (4) channels inside for cooling water passage, (5) channels on both sides for H_2 and O_2 distribution, (6) low gas permeability (<2×10^{-6} cm^3 s^{-1} cm^{-2}), (7) low electrical resistance (<10 mΩ cm^2), (8) high heat conductivity, (9) tough (>4 MPa) and flexible (3–5% deflection at mid-span) to reduce handling damage, (10) durable (good electrochemical stability, min. 5000 h for automotive use), (11) low cost ($6 kW^{-1}), and (12) high dimensional accuracy for uniform contact resistance. All of these requirements make the cost-effective design and manufacturing of bipolar plates a challenging research topic in addition to other research issues in fuel cells such as membrane, coating, catalyst, sealing, etc. developments.

The selection of material and geometry, and the development of fabrication methods for bipolar plates are ongoing research activities at various institutes and companies all around the world. In the past few years, the fabrication methods and material selection for bipolar plates in the proton exchange membrane fuel cells (PEMFCs) for vehicle applications has gradually evolved and narrowed to the following candidates: (1) machined graphite plates, (2) stamped or photo etched metal plates with and without coatings, (3) molded polymer–carbon composite, and (4) molded carbon–carbon material. Sample of different types of bipolar plates are shown in Fig. 1.

Graphite bipolar plates have been the choice of earlier pilot applications and tests because of the excellent chemical stability of graphite to survive in the fuel cell environment, and the excellent electrical conductivity to minimize the ohmic loss due to the contact resistance. However, because of (a) high material and manufacturing (machining) costs, (b) poor mechanical properties (low strength and flexibility), and (c) high porosity levels (leading to high permeability), the commercial use of graphite materials in fuel cells is found to be impractical in their current status of processing, manufacturing and use [8,5,9–11]. Metallic and composite bipolar plates offer several advantages over the conventional graphite plates; thus they found to be viable alternative options in PEMFCs [12–15,11]. The cost of bipolar plates is estimated to be only 15–30% of the stack cost with the use of metal or composite bipolar plates compared to 60–70% with graphite materials [16].

Polymer–graphite composite bipolar plates, generally composed of resins (thermoplastic or thermosetting polymer), and fillers (graphite) with or without fiber reinforcement, have been demonstrated in many studies to provide a similar performance to the traditional graphite plates (e.g. high corrosion resistance, low contact resistance, and lightweight) and with advantages in terms of low material and manufacturing (molding) cost, more freedom in flow-field design, and short cycle time (10 s) for mass production [5,16,17]. However, one major drawback of this technology comes from the low electrical conductivity of the polymer resins. Various research efforts were performed to increase the bulk conductivity of this type of bipolar plates to meet the target of 100 S cm^{-1} (DOE goal by 2010). These efforts to increase the electrical conductivity include the alignment process, the use of conductive-tier layer (CTL) method [2], the variation of the graphite content and powder size [18], the use of metal plate as the base of the polymer–graphite

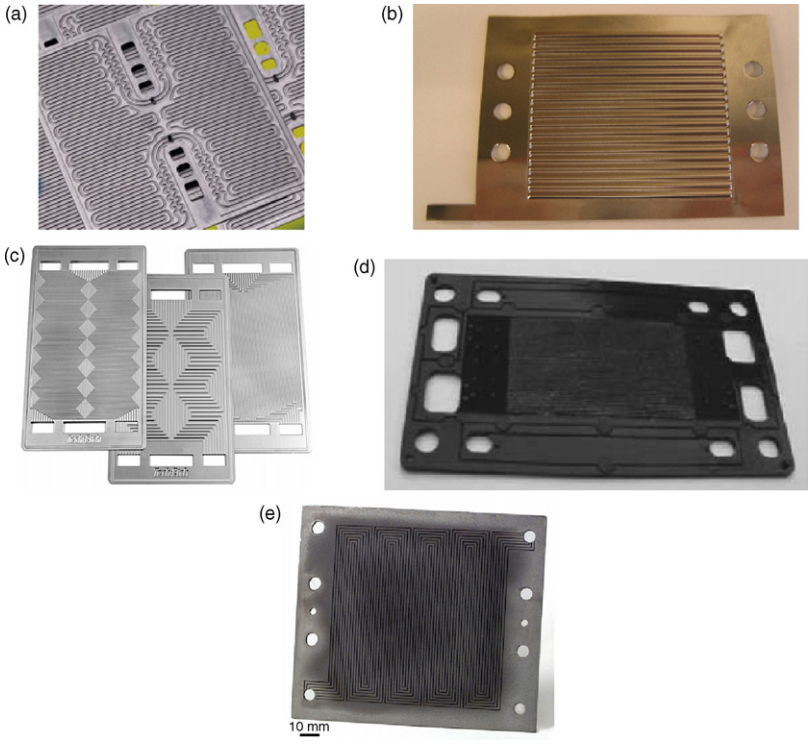

Fig. 1. Single bipolar plate of (a) machined graphite (Graftech Co.), (b) stamped stainless steel sheet (GenCell Corp.), (c) photo etched stainless steel/titanium plate (Tech-etch, Inc.), (d) molded polymer–carbon composite [5], and (e) molded carbon–carbon material [13].

composite (developed at Los Alamos National Laboratory) [7], and the use of metal coating [17]. Another issue concerning the composite bipolar plates is the low stack volumetric power density which is limited by the plate thickness that cannot be reduced below 1 mm by compression molding process (current composite plates are around 2–3 mm thick). In addition, it is very difficult to obtain accurate dimensions of the final plates from the molding process, and these dimensional variations in turn inevitably degrade the overall performance of the fuel cell stack. Injection molding was proposed for a better dimensional accuracy and short cycle time, but this technique has a higher mold wear and a limitation on the maximum thickness [5]. There are also concerns about the decrease in strength and stiffness of the polymer composite plates when operating at elevated temperature levels inside the PEMFCs [11]. Depending on the type of composites, the cost of these plates has been reported to be between \$5.4 and 40 kW^{-1} [5,17] or \$2.7–13.5 kg^{-1} [19], and the initial and long-term operation performance was shown to be comparable to that of the graphite plates [16,17].

Carbon/carbon composite bipolar plates, developed at Oak Ridge National Lab [13], are reported to have high electrical conductivity, high strength, lightweight, and low permeability. These plates are produced by slurry molding short carbon fibers into preform structures, molding features into the green body, and using chemical vapor infiltration (CVI) to strengthen the material, increase the conductivity, and densify the surface to make it impermeable. The complexity and the cost of the CVI process make this option inappropriate for the mass production [5,11].

Stainless steel bipolar plates have received considerable attention among metal bipolar plates due to their low cost, excellent mechanical, electrical, and thermal properties, and good manufacturability. Existing manufacturing methods of metallic bipolar plates include stamping of stainless steel sheets as shown in Fig. 1b, and photo etching of stainless steel/titanium plates as shown in Fig. 1c. However, the stainless steel bipolar plates are prone to corrosion and dissolution in the hazardous environment inside of the fuel cell which may lead to a possibility of metal ions damaging the MEA [11,7]. Therefore, a thin layer of coating is necessary to achieve the corrosion resistance target and to extend the fuel cell life [20,11,21,22,15]. Gold coating on SS316L plates had been demonstrated to provide similar performance to the graphite plates [15]. Thermal expansion of the base metals and the coating should be selected to be as close to each other as possible to avoid the formation of micro-pores/cracks. In addition, the coating should be applied in a defect-free fashion to avoid the original problem of membrane poisoning [7]. Recently, Brady et al. had developed a preferential thermal nitridation process to form pinhole free CrN/Cr_2N coating on Ni–Cr alloy [23]. Another vital issue is the interfacial contact resistance (ohmic losses) between the metallic bipolar plate and the carbon paper [24]. This resistance is increased due to the formation of the passive film that reduces the overall power output. The formation of these films varies depending on the elemental composition of the stainless steel alloy. The chromium content is also found to have a favorable influence on the anodic behavior [1,25,9,14].

Up to date, metal and composite bipolar plates are the two competing technologies for the commercialization of the PEMFCs in the near future with the polymer composite bipolar plates showing a slight potential edge over the metal plates due to the fact that some of the composite plates are now available in the market [7]. However, with the advancement in the surface coating technologies and suitable coating materials, metal bipolar plates can easily outperform the composite bipolar plates due mainly to its electrical and mechanical properties, leading to higher power efficiency, density, and durability. In this study, we proposed a novel manufacturing process for making of the metal bipolar plates from initially flat thin blanks using hydraulic pressure and in-die mechanical joining technique.

2. Description of the novel hybrid manufacturing process

In contrast to the existing methods of bipolar plate manufacturing, the novel hybrid process is expected to result in thin, lightweight, flexible bipolar plates with internal cooling channels, and flow fields (micro-channels) net-shape formed on both sides (anode and cathode) in one step and one die, thus eliminating handling, welding, assembly and sealing processes. Hence, the dimensional tolerances and surface quality will be improved leading to superior advantages and performance due to reduced variations in eventual assembly of the stacks and consistent contact resistance properties. The closest technology to the proposed one has been developed by Allen [20,26], where additional stamping steps are taken to form channels at both sides and middle as explained in their various publications and patents.

The novel hybrid manufacturing process introduced in this study is composed of the hydroforming of double thin sheet metal blanks to form micro-channels on both sides and mechanically joining them at various contact spots to create internal cooling channels. The process is depicted in Fig. 2, and can be explained as follows: two sheet metal blanks are placed between the upper and lower die halves, which have the intricate shape of micro-channels to be imprinted on the blanks. The dies are pushed against each other at the edges (i.e., periphery) of the sheet metal to provide sealing. Then, high pressure fluid is supplied between the blanks. The internal pressure forces the blanks to deform into the shape of the dies. Once the forming into complex micro-channels is completed or near completed, the upper and lower dies are further pressed against each other to generate a mechanical joint between two contacting surfaces of the sheet blanks to form the final shape of the bipolar plate. Finished bipolar plates with precisely formed internal cooling channels as well as micro-channels on anode and cathode sides would not only reduce the assembly operations but also would make the handling of the plates during assembly easier and safer and lead to much less variation.

With this method, efficient material utilization can be achieved resulting in thinner bipolar plates with integrated cooling channels, sealing and manifolds. Total thickness of the bipolar plates in the existing methods can go up to 4 mm. Using

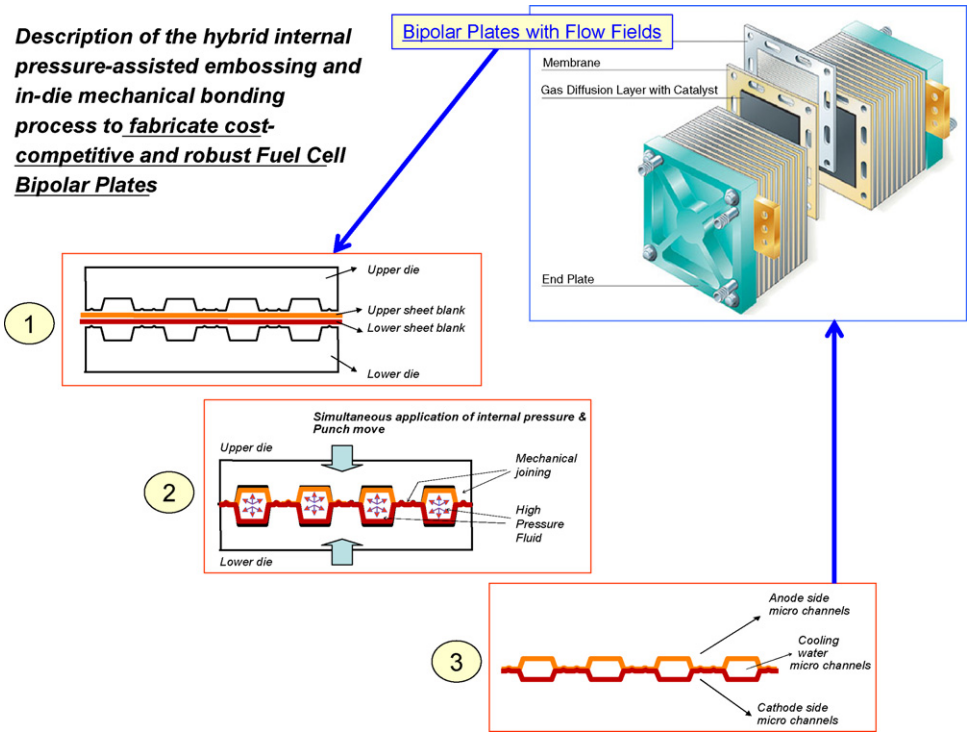

Fig. 2. The conceptualized hybrid manufacturing process.

this technique, thin blank sheet materials can be formed into integrated bipolar plates with a total thickness of less than 1 mm. As a result, it will be possible to improve the power density up to the required levels of 1 kW kg^{-1} (DOE goal 2010), while reducing the stack cost and increasing the service life.

To justify the potential of the hybrid method as a solution to reduce the cost of the bipolar plate down to meet the DOE goal of \$6 kW^{-1} by year 2010, a cost estimation was carried out for a double bipolar plate of non-coated SS304 with the size of 25 cm × 25 cm based on the following assumptions: (1) production rate = 1,000,000 double bipolar plates per year, (2) production time (loading, hydroforming, welding, and ejecting) = 12 s, (3) equipments and tooling cost per 1 production line = \$300,000, (4) labor cost = \$30 h^{-1}, (5) material cost of non-coated SS304 sheet = \$4.74 kg^{-1}, and (6) 20% depreciation cost and 30% indirect cost. The cost of making a double bipolar plate by this method is estimated to be \$2.60. In order to convert such cost estimation into a standard unit of \$ kW^{-1}, additional performance tests would be necessary. We plan to conduct such tests and estimations in the phases of this study.

In the following section, we demonstrate the feasibility of the conceptualized process and identify scientific and technological issues for further investigations. Specifically, two sets of experimental investigations were performed and presented: (1) hydroforming of thin sheet metal blanks into micro-channels, and (2) mechanical bonding (i.e., pressure welding) of thin sheet metal blanks. In the fourth section, we discuss the experimental results to reach some conclusions as summarized in the fifth section.

3. Experimental setup and methodology

3.1. Hydroforming of micro-channels

An experimental apparatus was designed and built for the hydroforming tests on thin sheet metal. The apparatus, as shown in Fig. 3, is composed of (1) upper die, (2) lower die, (3) three die inserts with micro-channels feature, (4) threaded bolts to provide clamping force between the upper and lower dies, (5) copper gaskets for sealing between the two die halves, (6) high pressure pump, and (7) thin sheet specimens. For all of the tests, the blank material is constrained at the periphery; thus, material is not allowed to flow into the die cavity. Three different micro-channel tool inserts were used to understand the limitations of fabricating multi-array, different size micro-channels.

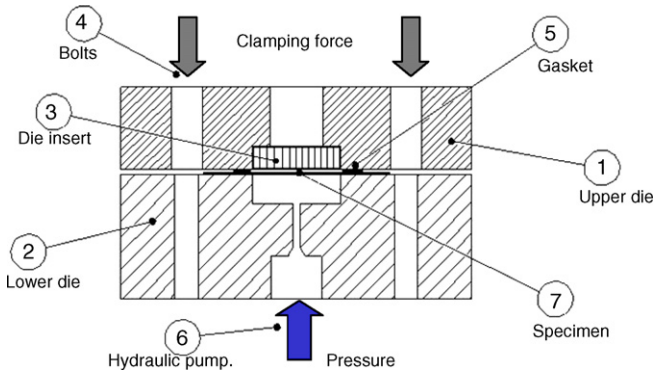

Fig. 3. Micro-channel hydroforming tooling.

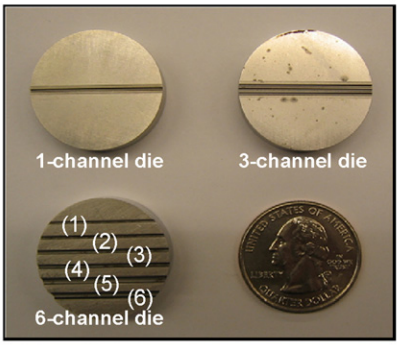

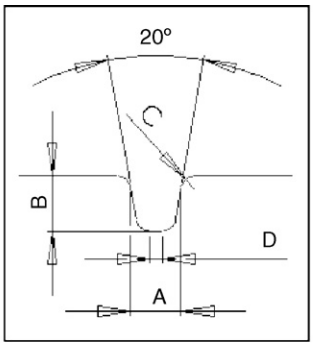

Dimensions of each die inserts [mm]								
Feature	1 Channel	3 Channels	6 Channels					
			#1	#2	#3	#4	#5	#6
A	0.46	0.46	0.52	0.63	0.78	0.78	1.33	1.33
B	0.50	0.50	0.15	0.24	0.24	0.46	0.46	0.98
C	0.13	0.13	0.13	0.13	0.13	0.13	0.26	0.26
D	0.11	0.11	N/A	N/A	N/A	N/A	N/A	N/A
Inter channel distance*	N/A	0.82	3.00	3.00	3.00	3.00	3.00	3.00

* Distance measured from center to center of adjacent channels
Note: All channels have 10 degree draft angle

Fig. 4. Detail geometry of micro-channels for three different die inserts.

Dimensional measurements using a laser scanning method were performed to characterize the formability of micro-channels at various aspect ratios under different internal pressure conditions.

Hydroforming of thin stainless steel 304 (SS304) blanks with a sheet thickness of 0.051 mm into micro-channels was performed using three different die inserts shown in Fig. 4. The first insert tooling has a single channel with 0.46 mm × 0.50 mm in width and height whereas in the second insert tooling, there are three channels of the same size with spacing between each channel (center-to-center distance) of 0.82 mm. Finally, in the third insert tooling, there are six channels of different micro-channels ranging from 0.52 to 1.33 mm in width and from 0.15 to 0.98 mm in height. Dimensions of micro-channels in these inserts are also shown in Fig. 4. For all micro-channels, the corner radius is 0.125 mm with a 10° draft angle.

3.2. Mechanical bonding of thin sheet metal blanks

Simple off-line tests were conducted using two sets of experimental apparatus. Fig. 5 shows the setup for (a) cold pressure welding process, and (b) warm pressure welding process (i.e., diffusion welding). Cold pressure welding test apparatus consists of upper and lower dies and two pins with the same diameter of 4.76 mm (3/16 in.). These pins were placed inside a straight groove located at the center of each die. To prevent distortion of the sheets from bending, two thin pieces of wood were placed beneath the specimens to assure the symmetry of the setup. The warm pressure welding test apparatus is similar, but with a pin diameter of 1.59 mm (1/16 in.) and ceramic ring heaters attached to each die. These heaters are capable of heating the die up to 760 °C (1400 °F). Since the pin diameter is relatively small, no supporting wood pieces were used to prevent bending distortion. Three different equipments, 3- and 10-t MTS machines and a 220-t Instron machine, were employed to supply the joining force.

4. Results and discussion

4.1. Hydroforming of micro-channels

Fig. 6 illustrates examples of the hydroformed micro-channel plates, which were formed at different pressure levels between 55.1 and 82.7 MPa (8000 and 12,000 psi). The profiles of the formed channels were measured using a laser beam measurement system. Examples of micro-channel profile measurement are depicted in Fig. 7. The results from the experiments revealed a very promising process potential in forming of the micro-channels. As expected, the percentage of the die filling increases with increased internal pressure and could be observed in Fig. 7a and b. The dimensional variation between different samples formed at the same pressure was found to be around 10–15 μm. Thus, we can conclude that process control and repeatability of

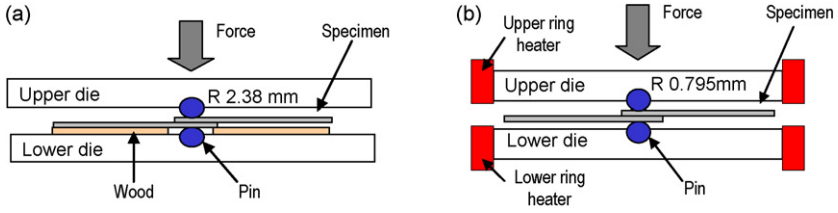

Fig. 5. Mechanical joining test apparatus for (a) cold pressure welding and (b) warm pressure welding.

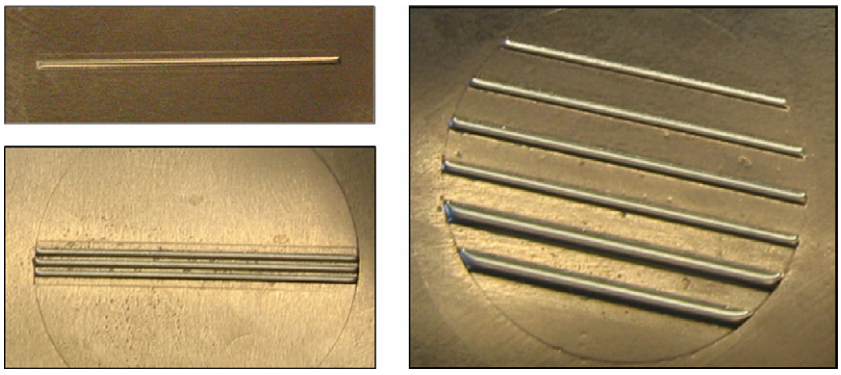

Fig. 6. Samples of hydroformed micro-channels using SS304, 0.051 mm thick.

the micro-channel hydroforming is reasonably good. The effect of inter-channel distance was observed that, at the same pressure level, the die filling was higher in the 1-channel die than the 3-channel die due to the constraining of the material flow in the latter case. Finally, the effect of channel shape and geometries on the formability is shown in the 6-channel specimens. It is shown in Fig. 7c that for a given channel size, there exists a maximum aspect ratio at which the sheet blank could be formed, and this value is mostly limited by the channel width. Future studies will include an in-depth investigation to determine optimal design of micro-channel considering both fluid flow/distribution for the reactants and manufacturability aspects.

4.2. Pressure welding of thin sheet metals

The first set of experiments was conducted in a cold pressure welding conditions. Thin sheets of SS316, Ni201, and Al3003 with thickness between 50 and 200 μm were cut into a size of 24 mm × 50 mm, and all specimen surfaces were degreased using acetone. The effects of material type, thickness, surface condition, and welding pressure on the solid-state bondability and bond strength were investigated in this experimental set.

The material properties and the experimental results are tabulated in Table 1. The minimum welding force, defined as the minimum force required to create bonding between the two spec-

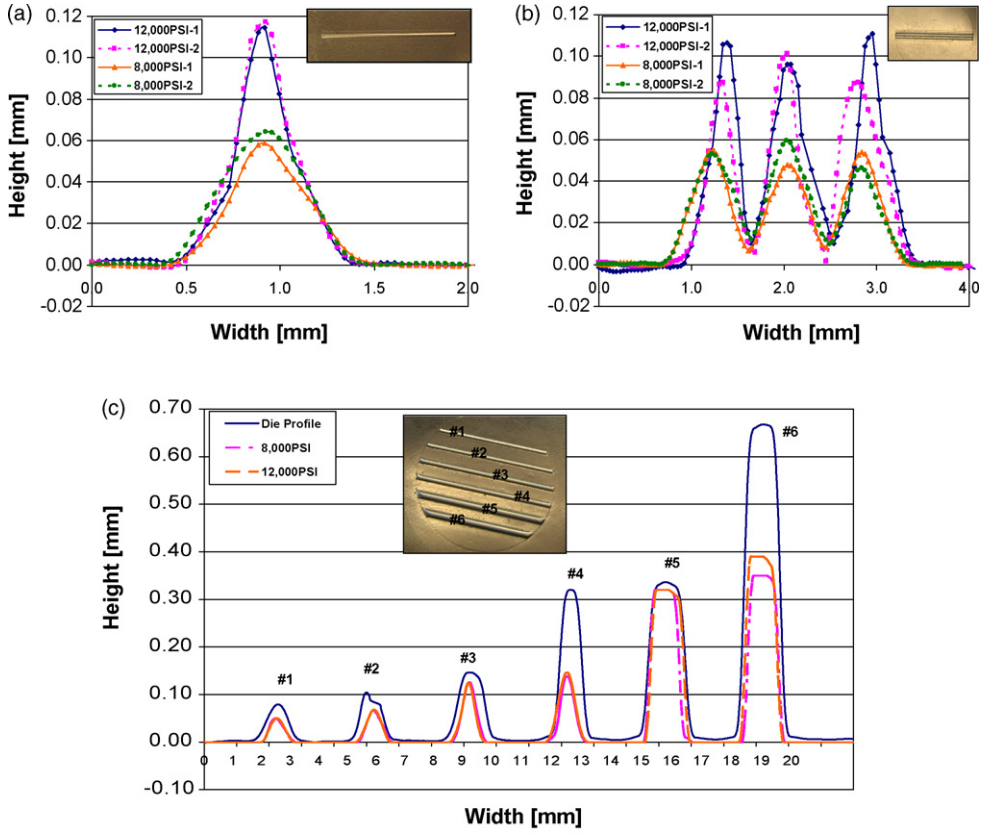

Fig. 7. Profiles of micro-channels measured by laser beam measurement system. (a) 1-Channel specimens; (b) 3-channel specimens; (c) 6-channel die and specimens.

Table 1
Material specification and experimental results

Grade	Thickness (mm)	YS (MPa)	Surface condition	Welding force (kN)	Max. shear force (N)	Thickness reduction ratio
Al3003	0.158	186	Wet	17.5[a]	28.6	0.84
				21.9	54.0	0.89
			Dry	15.6[a]	45.1	0.65
				18.7	71.7	0.72
				21.9	117.1	0.76
			Brushed	13.7[a]	86.0	0.67
				18.7	132.8	0.72
				21.9	188.0	0.74
Ni201	0.051	N/A	Dry	No weld	N/A	N/A
	0.127	652	Dry	40.0[a]	104.8	0.69
				55.1	137.6	0.76
				70.0	266.6	0.86
SS316	0.127	251	Brushed	No weld	N/A	N/A

[a] Minimum welding force.

imens, was determined based on a trial and error method. In this study, the bond quality was quantified by the maximum shear load that the bond can withstand before breaking. A 5-kN MTS machine with a pair of light-duty grippers was used for the tensile tests. For every test, the specimens were pulled at 0.05 mm s^{-1} and the bond strength was determined using the peak force recorded during the tensile tests. In addition, the thickness reduction ratio, defined as the ratio of the reduced thickness ($t_0 - t_f$) to the original sheet thickness (t_0), was used to define the amount of plastic deformation of the sheet blanks at the end of the stroke.

The effect of surface condition (wet, dry, and brushed) on minimum welding force and bond strength was investigated using Al3003 specimens. Water was used as the fluid medium to represent the wet surface condition, while coarse sandpaper (grit number 60, i.e., 60 abrasive particles per square inch) was used to prepare the brushed surface condition. To prevent an oxide layer from forming, the cleaning and brushing of the specimen surfaces were performed immediately before the welding. Based on the results shown in Table 1, the brushed surface reduced the minimum welding force and enhanced the bond strength, while the wet surface was shown to do the opposite. This trend agrees with the results reported in literature [27,28]. Since the surface condition directly affects the minimum welding force, it also has a direct impact on the threshold reduction ratio as shown in Table 1. This value was found to be approximately 65–85% for Al3003, depending on the surface conditions, and about 70% for Ni201. The reduction ratio was shown to increase with an increase in the welding force.

The effect of material type and thickness on the minimum welding force was studied using Al3003 and Ni201 blanks. For bonding to occur, the plastic deformation of the two metals is necessary. Therefore, the welding force or pressure must be sufficient enough to generate the plastic flow at the interface of the two metal plates. Since Ni201 has much higher yield strength than that of the Al3003, joining Ni201 would require much more force than joining Al3003 (40 kN for Ni201 and 15.6 kN for Al3003). On the other hand, SS316 could not be joined even with brushed surfaces and at the high welding force of 130 kN. At this level of welding force, the insert pins started to deform. In addition, the sheet thickness was shown to have a significant impact on the material flow. In a thinner sheet, there will be less of the material to be plastically deformed; thus, more welding force will be required to generate an adequate plastic flow at the contact interface. In this study, when the sheet thickness of Ni201

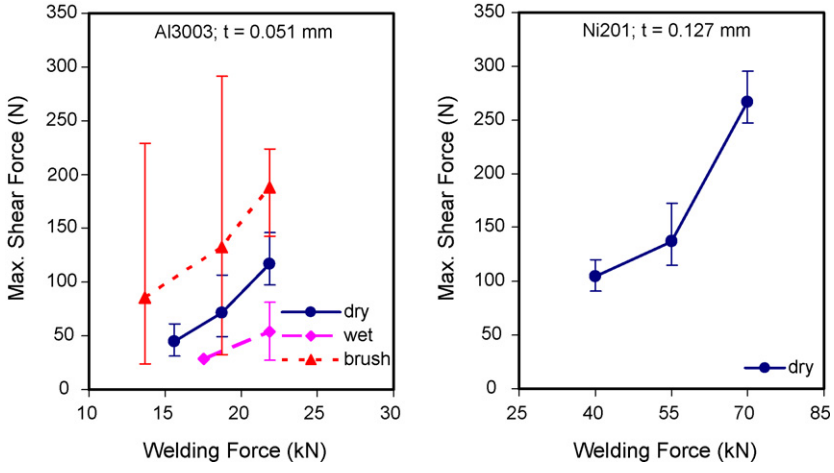

Fig. 8. Bond strength under shear loading.

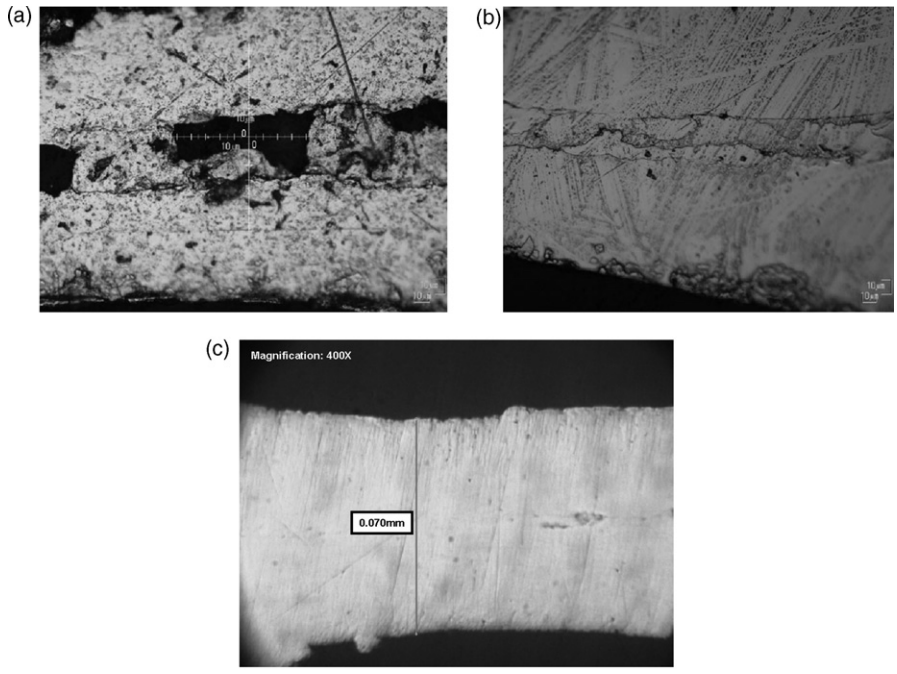

Fig. 9. Microscopic images of the welded specimens for (a) Al3003 and (b) Ni201 at room temperature, and (c) SS304 at 300 °C.

was reduced to 0.051 mm, unsuccessful joining was observed, even at the high welding force of 80 kN. The bond strength has been shown to increase with the welding force for Al3003 and Ni201, Fig. 8. A large variation in the maximum shear force values was observed for the brushed surface condition which might have been caused by an unequal amount of scratch brushing area at the contact interface between each specimen pair.

The microstructure of the bond formation area is shown in Fig. 9. For the Al3003 specimen, Fig. 9a, the bonding did not occur throughout the contact surface, instead taking place at certain spots where the material was pushed through the fractured layer of the contaminant films, showing that the result agrees with the 'film theory' [29]. The dark spots shown in Fig. 9a were regarded as oxide layers that still covered some sections of the contact interface of the two surfaces. On the other hand, no contaminant layer was observed in the case of Ni201, Fig. 9b, and bonding took place along the entire contact surface. This, in turn, resulted in a stronger bond than the Al3003 specimens where oxide layers were present.

The second set of experiments involved the pressure welding process at elevated temperature of sheet metals. Preliminary tests were conducted using the second die set as shown in Fig. 5b on stainless steel sheets since this material cannot be welded at a room temperature. Based on the experimental results, successful bonding of SS304 blanks with a thickness of 0.051 mm could be obtained at a welding force and temperature of 25 kN and 300 °C, respectively. A microscopic image of the welded area is shown in Fig. 9c. The bonding between the two blanks of SS304 took place along the entire contact interface with no sign of contaminant layers, which is similar to the case of bonding nickel specimens. At this force and temperature level, the thickness reduction ratio was calculated to be approximately 30%, which is much lower than the threshold reduction value of aluminum and nickel welded in the cold condition. The temperature is shown to have a significant impact in stimulating the plastic flow of the material at the interfaces; thus, reduces the thickness reduction ratio. Further investigation was carried out to study the effect of temperature on the bond strength. In doing so, SS304 blanks were welded at two different temperature levels under the same force condition (25 kN). Tensile tests were used to test the bond strength of the welded specimens. The test results are shown in Fig. 10 which reveals an obvious effect of temperature on the bond strength. The bond strength was found to be increased with the welding temperature. The effect of temperature on the bond formation mechanisms will be investigated and understood as a part of the future study. Nonetheless, it has been shown that SS304 blanks with thickness below 0.1 mm could be mechanically bonded under high compressive force in a warm condition.

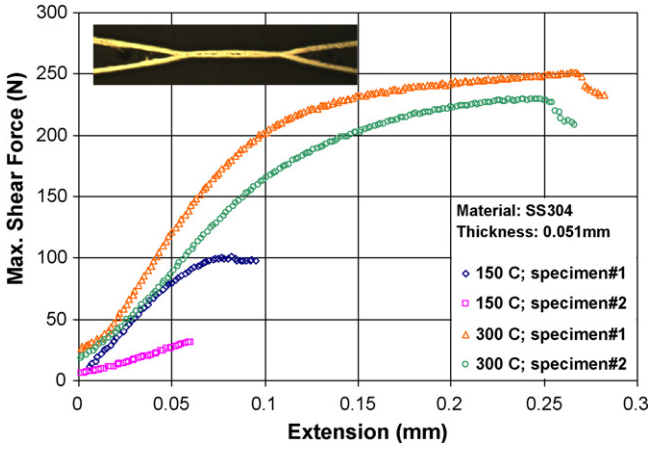

Fig. 10. Bond strength of bonded SS304 specimens.

5. Summary and conclusions

The results from this study revealed that the conceptualized novel hybrid manufacturing process is highly feasible for fabricating multi-array micro-channels on large surface area thin sheet metal blanks. It was also demonstrated that it was feasible to bond two thin sheet blanks using mechanical pressurizing at micro/meso-scale contact areas. The two sets of experiments conducted in this study, representing the actual forming and bonding conditions which will take place during the actual process, showed that SS304 blanks with thickness of 0.051 mm were successfully formed into various micro-channels dimensions by using internal pressure, and bonded together with reasonable strength (>200 N) by the warm pressure welding technique. In addition, it was shown that the presence of fluid medium and the effect of sheet thickness which cause some difficulties in joining of the blanks could be simply overcome by applying low amount of heating. With the sheet thickness values tested (0.051 mm), it will be very possible to produce double bipolar plates with the overall thickness below 1 mm in order to meet the power density requirement of 1 kW kg^{-1} in PEMFCs. The estimated cost of producing a double bipolar plate by the proposed method using a non-coated SS304 is $2.60. This cost is believed to meet the $6 kW^{-1} target, but will be decided based on the performance test results of these double bipolar plates. In the near future, we will attempt to perform hydroforming of micro-channels and mechanical bonding simultaneously in a single die and operation and conduct performance tests of these double bipolar plates in a fuel cell tester unit. All in all, the authors strongly believe that the propose method, along with the advancement of metal coating technology, will be the key solution to the cost-competitive and high power density requirements of the fuel cell stack due to the superior material properties of the metals over the composites and the low dimensional tolerances and the consistent contact resistance on the eventual assembly of the double bipolar plates fabricated by this technique in the single die and single operation as compared to the existing stamping/etching and joining of metal bipolar plates techniques.

Acknowledgements

The authors would like to acknowledge and thank the National Science Foundation (NSF) for the partial financial support on this project. It was partially supported by the NSF DMII 0500068 grant and by the NSF I/UCRC Program under NSF IIP-0638588. We also would like to recognize the assistance of Dr. Ho Choi at the beginning of this investigation.

References

[1] R. Bar-On, R. Kirchain, R. Roth, J. Power Sources 109 (1) (2002) 71–75.
[2] R.H. Blunk, D.J. Lisi, Y.E. Yoo, C.L. Tucker, AIChE J. 49 (2003) 18–29.
[3] R.G. Kumar, G. Reddy, J. Power Sources 113 (2003) 11–18.
[4] T.E. Lipman, J.L. Edwards, D.M. Kammen, Energy Policy 32 (2004) 101–125.
[5] E. Middelman, W. Kout, B. Vogelaar, J. Lenssen, E. De Waal, J. Power Sources 118 (1–2) (2003) 44–46.
[6] X. Li, I. Sabir, Int. J. Hydrogen Energy 30 (2005) 359–371.
[7] A. Hermann, T. Chaudhuri, P. Spagnol, Int. J. Hydrogen Energy 30 (2005) 1297–1302.
[8] J. Scholta, et al., J. Power Sources 84 (2) (1999) 231–234.
[9] V. Mehta, J.S. Cooper, J. Power Sources 114 (1) (2003) 32–53.
[10] K. Jayakumar, S. Pandiyan, N. Rajalakshmi, K.S. Dhathathreyan, J. Power Sources 161 (2006) 454–459.
[11] B. Cunningham, D.G. Baird, J. Mater. Chem. 16 (2006) 4385–4388.
[12] M. Abdelhamid, Y. Mikhail, Proceedings of the Annual Conference of the American Institute of Chemical Eng., New Orleans, LA, March 13, 2002.
[13] T. Besmann, J. Henry, E. Lara-Curzio, J.W. Klett, D. Haack, K. Butcher, Proceedings of the Materials Research Society Symposium, vol. 756, 2003, pp. 415–422.
[14] H. Wang, M.A. Sweikart, J.A. Turner, J. Power Sources 115 (2) (2003) 243–251.
[15] J. Wind, R. Spah, W. Kaiser, G. Boehm, J. Power Sources 105 (2002) 256–260.
[16] E.A. Cho, U.-S. Jeon, H.Y. Ha, S.-A. Hong, I.-H. Oh, J. Power Sources 125 (2004) 178–182.
[17] M.H. Oh, Y.S. Yoon, S.G. Park, Electrochim. Acta 50 (2004) 777–780.
[18] H. Kuan, C.M. Ma, K. Chen, S. Chen, J. Power Sources 134 (2004) 7–17.
[19] A. Heinzel, F. Mahlendorf, O. Niemzig, C. Kreuz, J. Power Sources 131 (2004) 35–40.
[20] J.P. Allen, 2000 Fuel Cell Seminar Abstracts, 2000, pp. 55–58.
[21] L. Gladczuk, C. Joshi, A. Patel, J. Gurheen, Z. Iqbal, M. Sosnowski, Proceedings of the Materials Research Society Symposium, vol. 756, 2003, pp. 423–428.
[22] M.C. Li, C.L. Zeng, S.Z. Luo, J.N. Shen, H.C. Lin, C.N. Cao, Electrochim. Acta 48 (12) (2003) 1735–1741.
[23] M.P. Brady, B. Yang, H. Wang, J.A. Turner, K.L. More, M. Wilson, F. Garzon, JOM 58 (8) (2006) 50–57.
[24] Y.H. Lai, D. Miller, C. Ji, T. Trabold, Proceedings of the Second International Conference on Fuel Cell Science, Eng. and Tech., 2004.
[25] N. Cunningham, et al., J. Electrochem. Soc. 149 (7) (2002) A905–A911.
[26] J.P. Allen et al., US Patent # 6,777,126 (2004).
[27] N. Bay, Met. Constr. J. 18 (6) (1986) 369–372.
[28] N.D. Lukaschkin, A.P. Borissow, J. Mater. Process. Technol. 61 (1996) 292–297.
[29] W. Zhang, N. Bay, CIRP Ann.: Manuf. Technol. 45 (1) (1996) 215–220.